Hydrogen absorption properties of metal-ethylene complexes

W. Zhou,[1,2] T. Yildirim,[1,2,*] E. Durgun,[3,4] and S. Ciraci[3,4]
[1]*NIST Center for Neutron Research, National Institute of Standards and Technology, Gaithersburg, Maryland 20899, USA*
[2]*Department of Materials Science and Engineering, University of Pennsylvania, Philadelphia, Pennsylvania 19104, USA*
[3]*Department of Physics, Bilkent University, Ankara 06800, Turkey*
[4]*UNAM-National Nanotechnology Research Center, Bilkent University, Ankara 06800, Turkey*
(Received 23 January 2007; revised manuscript received 6 March 2007; published 30 August 2007)

Recently, we have predicted [Phys. Rev. Lett. **97**, 226102 (2006)] that a single ethylene molecule can form stable complexes with light transition metals (TMs) such as Ti and the resulting TM_n-ethylene complex can absorb up to ~12 and 14 wt % hydrogen for $n=1$ and 2, respectively. Here we extend this study to include a large number of other metals and different isomeric structures. We obtained interesting results for light metals such as Li. The ethylene molecule is able to complex with two Li atoms with a binding energy of 0.7 eV/Li which then binds up to two H_2 molecules per Li with a binding energy of 0.24 eV/H_2 and absorption capacity of 16 wt %, a record high value reported so far. The stability of the proposed metal-ethylene complexes was tested by extensive calculations such as normal-mode analysis, finite temperature first-principles molecular-dynamics (MD) simulations, and reaction path calculations. The phonon and MD simulations indicate that the proposed structures are stable up to 500 K. The reaction path calculations indicate about 1 eV activation barrier for the TM_2-ethylene complex to transform into a possible lower energy configuration where the ethylene molecule is dissociated. Importantly, no matter which isometric configuration the TM_2-ethylene complex possesses, the TM atoms are able to bind multiple hydrogen molecules with suitable binding energy for room-temperature storage. These results suggest that co-deposition of ethylene with a suitable precursor of TM or Li into nanopores of light-weight host materials may be a very promising route to discovering new materials with high-capacity hydrogen absorption properties.

DOI: 10.1103/PhysRevB.76.085434 PACS number(s): 68.43.Bc, 81.07.−b, 84.60.Ve

I. INTRODUCTION

The success of future hydrogen and fuel-cell technologies is critically dependent upon the discovery of new materials that can store a large amount of hydrogen at ambient conditions.[1–3] Recently, from quantum-mechanical calculations we found that the C=C bond in a single ethylene molecule, similar to C_{60} and carbon nanotubes,[4–8] can form a stable complex with transition metals (TMs) such as Ti.[9] The resulting TM_2-ethylene complex attracts up to ten hydrogen molecules via the Dewar-Kubas interaction,[10] reaching a gravimetric storage capacity of ~14 wt %.[9] The interaction between hydrogen molecules and transition metals lies between chemisorption and physisorption, with a binding energy of ~0.4 eV/H_2 compatible with room-temperature desorption or absorption at ambient conditions (i.e., at room temperature and under 1 atm. H_2 pressure).[3]

Different from metal decorated C_{60} or nanotubes, metal-C_2H_4 complexes are actually existing structures and have been actively studied in the past several decades, with the major goal being to understand the catalytic mechanisms and processes of metals. Experimental spectroscopic data on various complexes, such as Li, Mg, Al, and TMs complexed with C_2H_4, widely exist in the literature.[11–14] These complexes were typically synthesized by direct reaction of metal atoms with C_2H_4/Ar in the gas phase. Early theoretical studies[14–18] showed that the metal-C_2H_4 binding mechanisms could be either electrostatic (e.g., C_2H_4-Al), or Dewar-Chatt-Duncanson bonding (e.g., most C_2H_4 TMs). The ability of metal-C_2H_4 complexes to absorb H_2 was realized and investigated in our recent work.[9]

Here we extend our earlier work[9] and present a detailed theoretical study of the hydrogen absorption on a large number of metal-C_2H_4 complexes, including TMs and the alkali-metal Li. We organize the paper as follows. In the next section, we describe the computational methodology. In Sec. III, we discuss C_2H_4M complexes, various isomers of $C_2H_4M_2$ complexes, and present the metal binding energies, zero-temperature dynamics of these complexes and their hydrogen absorption properties (including the H_2 binding energies and maximum number of H_2 that the complex can absorb). In Sec. IV, we discuss the possible reaction paths (i.e., minimum-energy paths) and the activation energies (i.e., barriers) between various isomers of $C_2H_4Ti_2$ complexes. We also discuss an interesting catalytic effect of Ti, similar to the "spillover effect," where a molecularly bound H_2 molecule is first dissociated over Ti and then one of the H atoms is bonded to carbon, forming a CH_3 group. The resulting molecule is isostructural to an "ethanol" molecule and thus called "titanol." The titanol molecule is also able to absorb up to five H_2 as molecules with a binding energy of ~0.4 eV/H_2 and provide another interesting possibility for high-capacity hydrogen storage materials. In Sec. V, we present high-temperature first-principles molecular-dynamics (MD) studies on selected structures. Due to the small system size, we are able to carry out MD simulations up to 10 ps. We show that the proposed complex structures are quite stable and exhibit constructive desorption upon heating without destroying the underlying complex. Our concluding remarks are presented in Sec. VI.

 ©2007 The American Physical Society

II. DETAILS OF CALCULATIONS

Our first-principles energy calculations were done within density-functional theory using Vanderbilt-type ultra soft pseudopotentials with Perdew-Burke-Ernzerhof exchange correlation, as implemented in the PWSCF package.[19] We note an unfortunate typographical error in our previous paper[9] where "Perdew-Zunger" should actually be "Perdew-Burke-Ernzerhof." Single molecular complexes have been treated in a supercell of $20\times20\times20$ Å with Γ k-point and a cutoff energy of 408 eV. The structures are optimized until the maximum force allowed on each atom is less than 0.01 eV/Å for both spin-paired and spin-relaxed cases. The reaction path calculations were carried out using the nudged elastic band (NEB) method.[20,21] We used a total of 21 images between the reactant and the product, which were fully optimized during the NEB calculations. The MD simulations were carried out within the microcanonical ensemble (NVE) starting with the optimized structure and random initial atom velocities.[22,23] More details of the MD calculations are given in V.

III. STRUCTURAL, ELECTRONIC, AND DYNAMICAL PROPERTIES OF $C_2H_4M_n$ AND $C_2H_4M_n$-H_x COMPLEXES

We start by examining various possible configurations of $C_2H_4M_n$ complexes and their corresponding H_2 absorption properties. We consider both transition metals and light metal Li, and focus on $n=1$ and $n=2$ cases. Complexes with $n>2$ are less attractive for hydrogen storage due to potentially lower capacities and thus are not discussed here and should be avoided in the syntheses.

When one metal atom binds to the ethylene molecule, the configuration shown in Fig. 1(a) is the most energetically favorable one, where the metal atom forms a symmetric bridge "bond" with the C═C bond of ethylene. When two metal atoms bind to C_2H_4, the complex may adopt several possible configurations. In our initial study,[9] we focused on the sandwich structure [Fig. 1(b)]. Here we consider two additional isomeric structures: dimer par [Fig. 1(c)] and dimer perp [Fig. 1(e)]. In the sandwich configuration, each M atom is closer to one of the carbon atoms, leading to two different M-C "bonds." Note that for most transition metals (e.g., Ti), there is no classical chemical covalent bonding between the metal atom and carbon atom. The calculated bond population is found to be nearly zero for these metals. The slight shift of the metal atoms towards different C atoms only results in a minute contribution of the M-C covalentlike bond to the overall binding. In just a few cases (e.g., Fe), the metal and carbon atom are bonded more traditionally by a covalent bond, as shown in Fig. 1(d). For this reason, we generally specify these $C_2H_4M_n$ structures as "complexes" instead of "molecules."

The binding mechanism of the $C_2H_4TM_n$ complex has been discussed in detail in our previous work.[9] Essentially, the bonding orbital for the TM atoms and C_2H_4 results from the hybridization of the lowest-unoccupied molecular orbital (LUMO) of the ethylene molecule and the TM-d orbitals, in accord with Dewar coordination. For Li, the binding mechanism is different. In Fig. 2, we show the electronic density of states of the C_2H_4 molecule, the Li atom, and the C_2H_4Li complex. Projection analysis of the states indicates that the electron in the 2s state of Li is divided into two halves that are transferred to the LUMO of C_2H_4 and the 2p of the Li

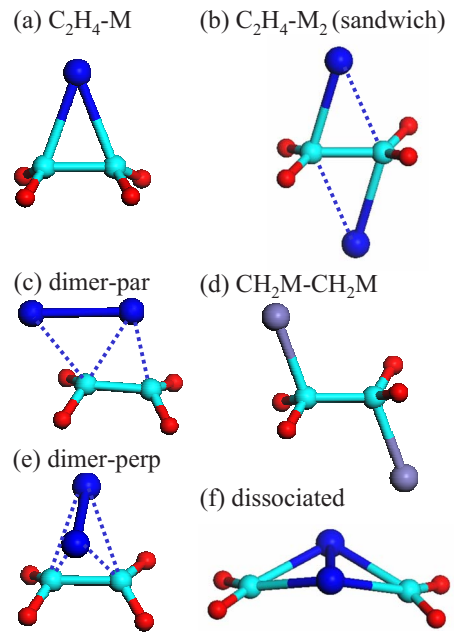

FIG. 1. (Color online) Various configurations of $C_2H_4M_n$ ($n=1$ and 2) complexes considered in this study. (a) C_2H_4 complexed with one metal atom. (b)–(e) C_2H_4 complexed with two metal atoms with different metal binding sites. Note that the bond-stick model is only used for clarity and should not be considered as an implication of the chemical covalent bonding between those atoms. For most metals, there is no classical chemical covalent bonding between the metal and carbon atoms. For a few metals (e.g., Fe), the complexes possess a structure, where M and C are bonded more traditionally by covalent bonding, as shown in (d). (f) $C_2H_4M_2$ complex with dissociated C═C bond. Large, medium, and small balls represent M, C, and H atoms, respectively.

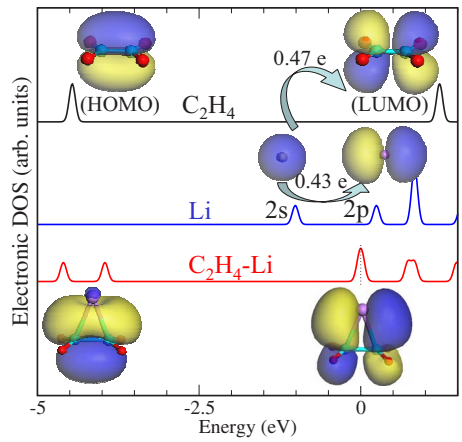

FIG. 2. (Color online) Electronic density of states of C_2H_4, Li atom, and C_2H_4+Li complex. The isosurfaces of the relevant molecular orbitals are also shown. The hybridization of the Li-2p state and the LUMO of C_2H_4 is apparent. See text for further explanation.

TABLE I. The metal-C_2H_4 binding energies (in eV/M atom) with respect to atomic and bulk energies of various metals, and the average H_2 binding energies (in eV/H_2) on C_2H_4M for various absorption configurations (see Fig. 3). The maximum number of H_2 molecules bonded to each metal is also shown.

Property/M	Li	Sc	Ti	V	Cr	Mn	Fe	Co	Ni	Cu	Zn	Zr	Mo	W	Pd	Pt
E_B (M atomic)	0.32	1.39	1.45	0.94	0.18	0.51	0.92	1.39	0.91	0.80	none	1.91	1.02	1.71	1.95	2.52
E_B (M bulk)	−1.41	−2.72	−3.68	−4.30	−3.44	−3.06	−1.64	−2.43	−1.99	−2.86		−4.23	−5.19	−6.65	−1.86	−2.82
E_B (per H_2), MH_2		0.96	1.16	1.00	0.01	0.59	1.01	0.94	1.13	0.19		1.90	0.85	1.80	0.83	1.33
E_B (per H_2), $M+H_2$	0.29	0.02	0.31	0.46	0.45							0.35	0.49	0.59	0.64	
max H_2/M	2	5	5	5	5	5	5	3	2	2		5	5	5	2	2
E_B (per H_2), $M+2H_2$	0.28								0.42	0.33					0.27	0.25
E_B (per H_2), MH_2+3H_2		0.40	0.54	0.66	0.34	0.24	0.31					0.78	0.61	0.85		
E_B (per H_2), $M+5H_2$		0.28	0.46	0.53	0.21	0.18	0.34					0.54	0.64	0.79		

atom, respectively. Then the $2p$ orbital of Li and the LUMO of C_2H_4 are hybridized for the binding of Li on the C_2H_4. From the isosurfaces of the molecular orbitals (also shown in Fig. 2), it is clear that the molecular orbital of C_2H_4Li near the zero energy (i.e., the Fermi energy) is a superposition of the LUMO of C_2H_4 and the p orbital of the Li atom. Also note that the occupied orbital of the C_2H_4Li complex at around −4 eV is about the same as that of the highest occupied molecular orbital (HOMO) of bare C_2H_4, except that there is a hole in the upper portion of the orbital due to the Li ion. The bond analysis does not show any covalent bonding between C and Li atoms. For $C_2H_4Li_2$, we observed also a binding mechanism similar to that of C_2H_4Li.

The metal binding energies on ethylene are summarized in Table I and Table II for one metal and two metal complexes, respectively. They are calculated by subtracting the equilibrium total energy E_T of the $C_2H_4M_n$ complex from the sum of the total energies of free molecular ethylene and of the M atom: $E_B(M)=[E_T(C_2H_4)+nE_T(M)-E_T(C_2H_4M_n)]/n$. According to the $E_B(M\text{-atomic})$ values shown in both tables, most TMs that we studied are able to bind relatively strongly to a C_2H_4 molecule, except Cr and Zn. In Table I, the variation of the TM binding energy with the number of TM-3d electrons displays a behavior similar to what was observed previously for the chemisorption of TMs on the surface of a single-walled carbon nanotube.[24,25] Namely, there exist two energy maxima between a minimum that occurs for the element with five d electrons. Table I also gives the binding energies with respect to bulk metal energies [$E_B(M$ bulk)] while Table II also gives E_B with respect to metal dimer energies [$E_B(M$ dimer)]. Note that all $E_B(M$ bulk) values are negative, indicating endothermic reactions. Apparently, metal atoms in vapor or some metal precursors, instead of bulk metals, are preferred when synthesizing these complex structures.

We next studied the H_2 storage capacity of the metal-ethylene complex, by calculating the interaction between $C_2H_4M_n$ and a different number of H_2 molecules. We considered various configurations for the hydrogen absorption on a metal center, as shown in Fig. 3. The first H_2 molecule absorbed may either be in molecular form [Fig. 3(a)] or in dissociated form [Fig. 3(b)]. For most transition metals, it is possible to absorb more, up to five H_2 per M atom. Two of the many possible multiple H_2 absorption configurations are shown in Figs. 3(c) and 3(d). For Li, in both C_2H_4Li and $C_2H_4Li_2$ complexes, each Li can bind to two H_2, resulting in absorption capacity of 10.3 and 16.0 wt %, respectively. The optimized configurations and structural parameters are shown in Fig. 4.

The nature of the metal-H_2 interaction is easy to understand. For TMs, since the bonding orbitals are mainly between metal d- and hydrogen σ^*-antibonding orbitals, the mechanism of this interesting interaction can be explained by the Kubas interaction.[10] For Li, the metal-H_2 binding is mainly electrostatic. We summarize the average H_2 binding energy for C_2H_4M in Table I. Note that the H_2 binding energies for the C_2H_4M complexes differ slightly from those given in our earlier work[9] for the $C_2H_4M_2$ complexes with the sandwich structure, a result of the slightly different electronic structures of the M atoms in the two types of complexes. Nevertheless, in most cases, the H_2 binding energies

TABLE II. The metal-C_2H_4 binding energies (in eV/M atom) of three isomeric $C_2H_4M_2$ configurations (see Fig. 1), with respect to atomic and dimer energies of various metals.

Property/M	Li	Sc	Ti	V	Cr	Mn	Fe	Co	Ni	Cu	Zn	Zr	Mo	W	Pd	Pt
E_B (M atomic), sandwich	0.69	1.39	1.47	1.21	0.05	0.37	0.83	1.30	0.70	1.41	none	1.69	0.37	1.18	1.56	1.78
E_B (M atomic), dimer par	0.54	1.77	2.02	1.62	0.10	0.64	1.65	1.63	1.09	1.34	none	2.66	2.20	3.26	1.88	2.61
E_B (M atomic), dimer perp	0.61	1.72	2.12	1.97	0.21	0.51	1.22	1.50	1.00	1.24	none	2.70	2.10	2.41	1.39	1.53
E_B (M dimer), sandwich	0.20	0.58	0.17	−0.21	0.79	0.33	−0.36	−3.45	−0.01	0.17		−0.10	−1.71	−1.30	0.75	0.20
E_B (M dimer), dimer par	0.05	0.96	0.72	0.20	0.84	0.60	0.46	−3.12	0.38	0.10		0.87	0.12	0.78	1.08	1.03
E_B (M dimer), dimer perp	0.12	0.91	0.82	0.54	0.95	0.47	0.03	−3.25	0.29	0.00		0.91	0.02	−0.07	0.58	−0.05

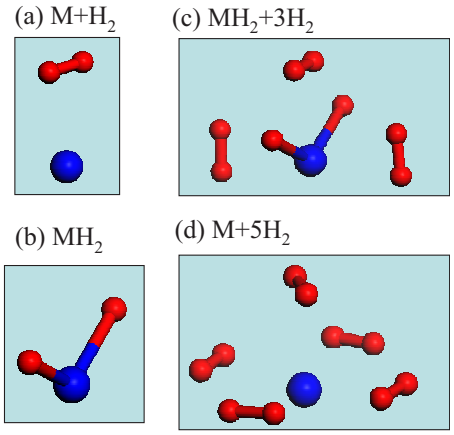

FIG. 3. (Color online) Various configurations that we considered in this study, for the hydrogen absorption on a metal center of a $C_2H_4M_n$ complex: (a) one H_2 absorbed molecularly; (b) H_2 dissociating with two M-H bond formed; (c) two atomic H and three H_2 molecules; (d) five H_2 absorbed as molecules. Large and small balls represent M and H atoms, respectively.

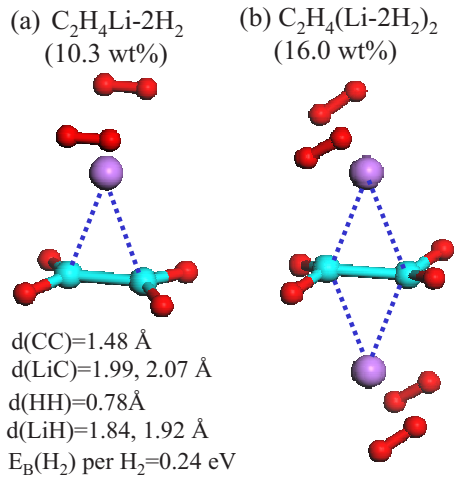

FIG. 4. (Color online) Hydrogen absorption configurations on (a) C_2H_4Li and (b) $C_2H_4Li_2$ complexes. Note that in both cases, each Li can bind two H_2, resulting in high absorption capacities. Large, medium, and small balls represent Li, C, and H atoms, respectively.

have the right order of magnitude for room-temperature storage. Since the hydrogens are mainly absorbed molecularly, we also expect fast absorption and desorption kinetics.

In order to test their stability, we further studied the dynamic of the $C_2H_4M_n$ complexes by normal-mode analysis. We found no soft (i.e., negative) mode, indicating that the complex structures are stable. Characteristic phonon modes are summarized in Table III, using Li and Ti as examples. Our calculated mode frequencies for the C_2H_4 molecule agree very well with the experimental values.[26] Metal binding to C_2H_4 elongates and thus softens the C═C bond, resulting in lower stretching mode frequencies. Also the softening of the CH_2-torsion and CH_2-bending modes is obvious. There are three main M-related vibrational modes. In two of these modes, M atoms vibrate parallel and perpendicular to the C═C bond. In the third mode, metal atoms vibrate perpendicular to the C_2H_4 plane. These three modes are unique for the $C_2H_4M_n$ complex and therefore should be present in any Raman or IR spectra of a successfully synthesized material.

We also calculated the normal modes of $C_2H_4M_n$ complexes absorbed with H_2 and did not find any soft modes, indicating that the configurations that we considered indeed correspond to local-energy minima. Among many vibrational modes, we note that the H_2 stretching mode is around 330–420 meV for the absorbed H_2 molecules, significantly lower than ~540 meV for the free H_2 molecule. Such a shift in the mode frequency would be the key feature that can be probed by Raman or IR measurement to confirm a successful synthesis of the structures predicted here. In the lower energy range, there are many M-H modes that are unique to the complexes. To manifest the M-H dynamics, we show in Fig. 5 the phonon density of states of $C_2H_4Ti_n$-H_x complexes weighted by neutron cross sections (note that H has much larger neutron-scattering cross section than C and most metals). These plots can provide a useful comparison to experiments when trying to synthesize these materials.

IV. ACTIVATION ENERGIES AND REACTION PATHS BETWEEN DIFFERENT ISOMERS

The $C_2H_4M_n$ and $C_2H_4M_n$-H_x complexes can have several isomeric structures. It is important to know the relative stabilities of these isomers and their implications for the hydrogen absorption properties. We thus studied the activation energies and reaction paths between different isomers of $C_2H_4M_n$ complexes. Here we discuss representative results on M=Ti.

TABLE III. Characteristic mode frequencies (meV) for C_2H_4, $C_2H_4Li_n$, and $C_2H_4Ti_n$ complexes. Experimental values for C_2H_4 (from Ref. 26) are also shown. Note that the metal-C_2H_4 binding significantly softens the C═C stretching, CH_2-torsion, and CH_2-bending modes. The three main M modes give unique signatures for metal-C_2H_4 complexes.

Mode/complex	C_2H_4	C_2H_4, expt.	C_2H_4Li	$C_2H_4Li_2$	C_2H_4Ti	$C_2H_4Ti_2$
C═C stretching	202	201	184	172	170	167
CH_2 torsion	128	127	99	49	52	56
CH_2 bending	115–165	117–166	84–145	54–141	94–140	73–134
M vib, ∥C═C bond			38	40 (in phase), 66 (out of phase)	62	15 (in phase), 57 (out of phase)
M vib, ⊥C═C bond			37	22 (in phase), 65 (out of phase)	56	22 (in phase), 62 (out of phase)
M vib, ⊥C_2H_4 plane			40	38 (in phase), 74 (out of phase)	63	29 (in phase), 48 (out of phase)

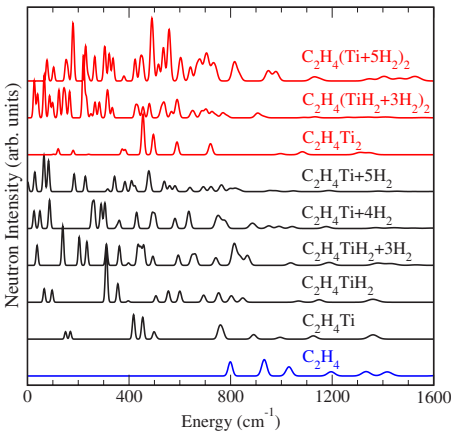

FIG. 5. (Color online) Simulated neutron inelastic spectrum for various $C_2H_4Ti_n$-H_x configurations. Note that the M-H dynamics are unique and can be used as a probe to identify these structures. Thus these plots can provide a useful comparison to experiments when trying to synthesize these materials.

We start with the $C_2H_4Ti+H_2$ complex and consider two possible structural transitions, which lead to lower energy configurations through the dissociation of an H_2 molecule over a Ti atom. In the first case, the H_2 molecule dissociates on top of the Ti atom. $C_2H_4(Ti+H_2)$ and $C_2H_4(TiH_2)$ are the reactant and product, respectively. Their relaxed structures correspond to the first and last images shown in the top panel of Fig. 6(a). The calculated minimum-energy path for this process gives ~0.25 eV barrier, which is small but still significant since the $C_2H_4(Ti+H_2)$ configuration corresponds to a local-energy minimum and possesses a H_2 binding energy of ~0.3 eV. In the second case, the H_2 molecule is first dissociated over Ti and then one of the H atoms goes to carbon, forming a CH_3 group. The activation energy plot for this process is shown in Fig. 6(b), indicating a very low barrier of only ~0.15 eV. Once the product [i.e., the last image of the top panel of Fig. 6(b)] forms, the CCTi-bond angle is very soft, resulting in the zero-temperature structure shown in the inset, which has only 30 meV lower energy than the product. The final structure of the molecule [Fig. 6(b), inset] is isostructural to the "ethanol" molecule and therefore we call it "titanol."

Since the titanol molecule is fairly easy to form, it is important to check if this new complex still possesses the high-capacity H_2 absorption property. In Fig. 7, we show several stable hydrogen absorption configurations on a titanol molecule. With only one H_2, it can be absorbed molecularly [Fig. 7(a)] with a bind energy of 0.3 eV or absorbed dissociatively [Fig. 7(b)], yielding a TiH_3 structure, with a binding energy of about 1.0 eV/H_2. We expect that the dissociation process may have a similar barrier to that found in Fig. 6(a). Importantly, the titanol molecule can bind up to five H_2 as molecules [Fig. 7(c)] with an average binding energy of ~0.4 eV/H_2.

Next, we study the $C_2H_4M_2$ dimer structures. For Ti, the dimer-perp structure [Fig. 8(a)] has lower total energy than the isomeric sandwich structure [Fig. 1(b)] and dimer-par structure [Fig. 1(c)]. Figure 8(c) shows the activation barrier for the transition from the sandwich configuration to the dimer-perp configuration. The activation energy is about 0.55 eV. Shown in Fig. 8(b) is one of the stable configurations that we identified for the hydrogen absorption on the $C_2H_4Ti_2$ dimer-perp structure. Apparently, regardless which isomer of $C_2H_4Ti_2$ that we have, the complex is always able to bind multiple hydrogen molecules.

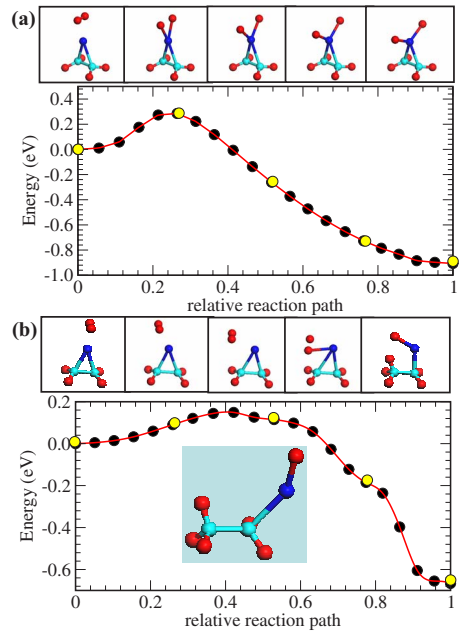

FIG. 6. (Color online) (a) The minimum-energy path for the dissociation of the H_2 molecule over the Ti atom complexed with C_2H_4. An energy barrier of ≈0.25 eV is found for the dissociation. A total of 21 images were used in the NEB calculations, five of which are shown on the top. Marked circles in the potential plot are the points corresponding to these five images. (b) The activation energy plot for the formation of titanol-molecule from $C_2H_4Ti+H_2$ complex, indicating a very low barrier of ≈0.15 eV. Once the final product forms, the CCTi-bond angle is very soft, resulting in the zero-temperature structure shown in the inset.

Finally, one may ask whether it is possible for the metal to catalyze and dissociate the C_2H_4 molecule (i.e., break the C═C bond), forming a more stable structure as shown in Fig. 1(f). Our calculations show that the activation energies for a sandwich to dissociated C_2H_4 [Fig. 9(a)] and a dimer-perp to dissociated C_2H_4 configurations [Fig. 9(b)] are both large, ~1.1 eV. Thus it is very unlikely that the dissociation would happen under near ambient conditions. Interestingly, we found that even the dissociated structure can still absorb multiple H_2, in which case, the system is somewhat similar to a Ti metallocarbohedryne (met-car) cluster.[27,28]

V. FINITE-TEMPERATURE FIRST-PRINCIPLES MD SIMULATIONS

In order to further test the stability of the $C_2H_4M_n-H_x$ complexes and the relative strength of different interactions (such as M-C_2H_4 M-H_2 interactions) and to identify possible reaction paths, we have carried out extensive first-principles MD simulations in the microcanonical ensemble (NVE).[22,23] We emphasize that our purpose was not to obtain the desorp-

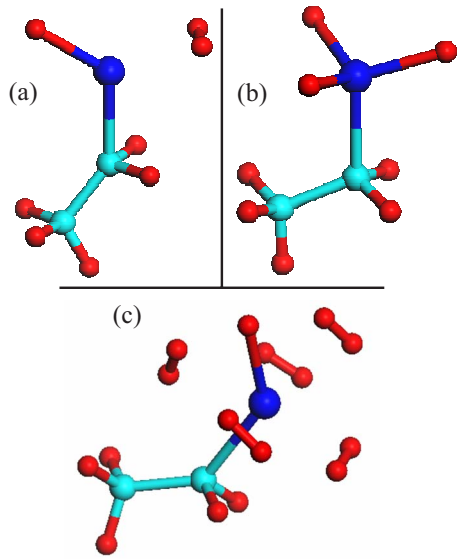

FIG. 7. (Color online) Hydrogen absorption on a titanol molecule. (a) One H_2 binds molecularly to Ti, with a binding energy of 0.3 eV. (b) One H_2 is dissociated, yielding TiH_3 structure. The corresponding binding energy is about 1.0 eV/H_2. (c) Five H_2 bind as molecules to the titanol molecule with an average binding energy of 0.4 eV/H_2. Large, medium, and small balls represent Ti, C, and H atoms, respectively.

tion temperature from the MD simulations, but rather to make sure that we are not missing other stable phases and to show that H_2-desorption can occur without destroying the underlying M-C_2H_4 complex.

The system is first optimized and then random initial velocities are generated to yield twice the target temperature.

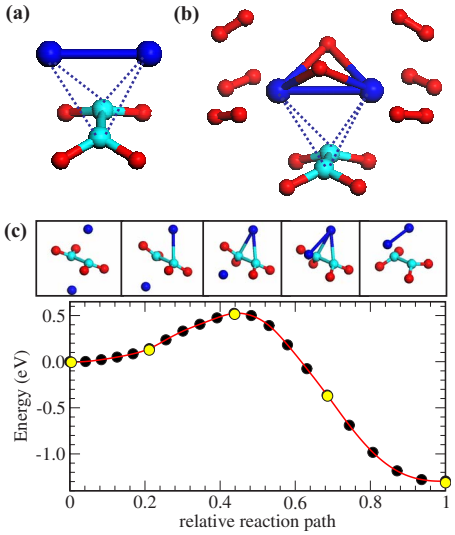

FIG. 8. (Color online) (a) Bare $C_2H_4Ti_2$ dimer-perp complex. (b) The complex with seven H_2 absorbed. Note that there also exists other stable configurations that not discussed here. (c) The minimum-energy path for the transition from $C_2H_4Ti_2$ sandwich configuration to dimer-perp configuration. The activation energy is about 0.55 eV. Note that regardless of which isomer of $C_2H_4Ti_2$ we have, the resulting complex is able to bind multiple hydrogen molecules.

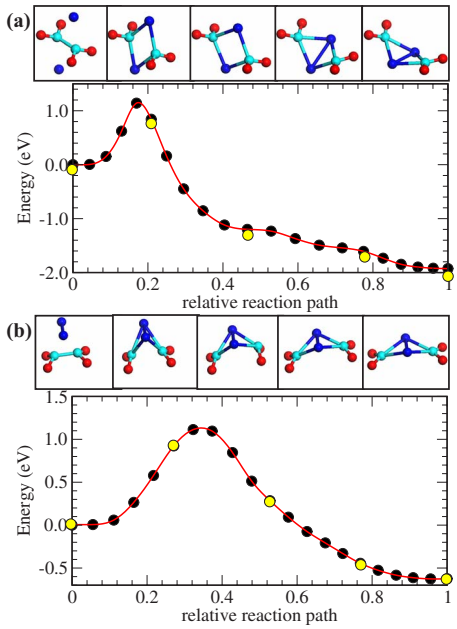

FIG. 9. (Color online) The minimum-energy paths for the transitions (a) from the $C_2H_4Ti_2$ sandwich to the dissociated configuration and (b) from $C_2H_4Ti_2$ dimer perp to the dissociated C_2H_4 configuration, respectively. In both cases, there are large energy barriers on the order of 1.1 eV.

When the system is in equilibrium, half of this energy goes to the potential and therefore the final temperature oscillates around the target temperature. We note that due to the small atomic mass of some elements (e.g., Li and H) in our system, it is essential to use a small MD time step such as 0.5 fs. Furthermore, convergence criteria for energy at each MD iteration should be very accurate (we used 10^{-7} eV) in order to avoid total energy/temperature drift (i.e., change in the total energy/temperature as a function of simulation time). Since we are studying an isolated molecular complex in free space, it is also important that we eliminate the six degrees of freedom (i.e., three rotations and three translations) of the molecule. When this is not done, we observed that the input temperature goes to totally uniform translation or/rotation of the molecules rather than populating the vibrational modes after 1–2-ps simulations. In our simulations, we fixed one of the carbon atoms and then two components of position of the other carbon atom and one component of M atom position (which prevents the rotation of the molecule in the CCM plane). In this way, the total degrees of freedom allowed in our simulation are $N_F = 3 \times (N-6)$, as expected for an isolated molecule. The temperature of the system is defined as $T(t) = \Sigma_i m_i v_i^2 / (2k_B N_F)$, where i runs over the atoms of the complex and k_B is Boltzmann's constant. The relative fluctuation is of the order of $1/\sqrt{N_F}$. We also note that since our system is very small (i.e., about a dozen atoms), it is basically a collection of a small number of harmonic oscillators and therefore temperature fluctuations are large. In fact, trying to control system temperature through velocity scaling[22,23] at a small time interval does not work and yields wrong results. The microcanonical ensemble is thus the best for our purpose and as we shall see below it works well

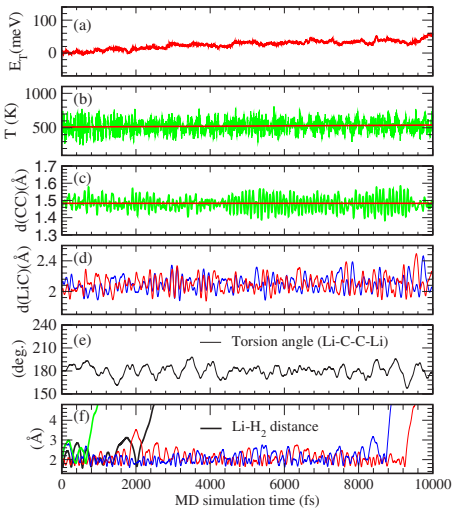

FIG. 10. (Color online) First-principles MD results at 500 K for the $C_2H_4Li_2+4H_2$ complex. Shown are the time evolution of various quantities, including total energy (a) and temperature (b) of the system, C-C (c) and Li-C (d) bond distances, and Li-C-C-Li torsion angle (e). The bottom panel (f) shows the distance between the Li atom and the hydrogen center of mass, indicating successive desorption of H_2 molecules along the simulation.

provided that a small time step is used and the total energy/force calculations are accurate enough. Here we present representative results on M=Li, Ti as examples.

Our MD results for $C_2H_4Li_2+4H_2$ at 500 K are summarized in Fig. 10. The constant of motion plot shows only 50-meV drift in total energy over 10-ps simulation time, which causes a small temperature drift. The C-C and Li-C distances, shown in Figs. 10(c) and 10(d) respectively, indicate that the bare $C_2H_4Li_2$ molecule is stable at this temperature. The torsion angle Li-C-C-Li shows no sign of Li-dimer formation and oscillates around 180°. The bottom panel in Fig. 10 shows the distance between Li atoms and the center of mass of H_2 molecules, indicating the successive release of hydrogen molecules from the system. The first H_2 leaves the system around 400 fs. The fluctuations in the distances become very large at 2000 fs, resulting from the release of another hydrogen molecule. Around 8–10 ps, the other two hydrogen molecules also leave the system. Even though with 10-ps MD simulations, it is not possible to get reliable temperatures; the results are still very promising and suggest that the $C_2H_4Li_2$ system can stay intact at 500 K while it releases four hydrogen molecules.

We next studied the stability of the $C_2H_4Ti_n$ system. We performed MD simulations up to 10 ps on $C_2H_4Ti_2$ (sandwich), $C_2H_4Ti+H_2$, $C_2H_4(Ti+5H_2)_2$ (sandwich), and the titanol molecule (CH_3CH_2TiH) at 300 and 500 K. In the simulations on the two metal sandwich systems, we did not observe any Ti-dimer formation. In the case for $C_2H_4Ti+H_2$, we did observe the spill-over effect, where the H_2 is dissociated over Ti and C and then Ti moved away with one hydrogen atom attached to it. This is essentially the titanol formation process that we discussed in the previous section.

The MD results for the $C_2H_4(Ti+5H_2)_2$ system at 500 K are summarized in Fig. 11. During the 10-ps simulation time,

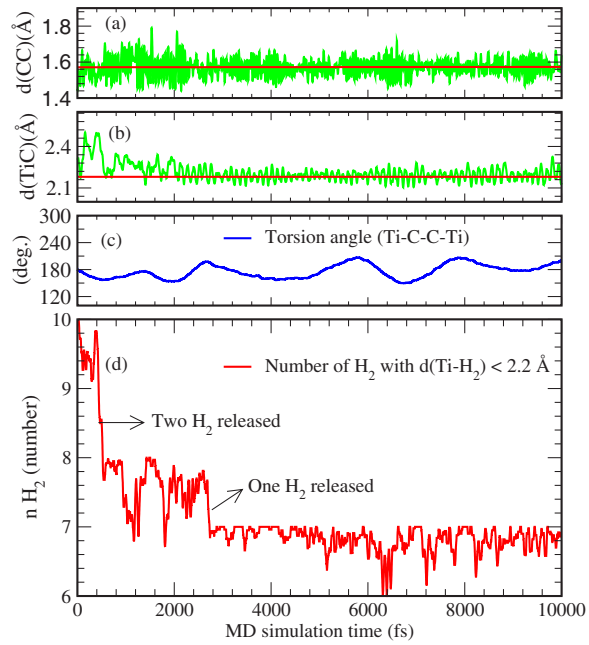

FIG. 11. (Color online) First-principles MD results at 500 K for the $C_2H_4(Ti+5H_2)_2$ sandwich complex. Various quantities are shown, including C-C (a) and Ti-C (b) bond distances, and Ti-C-C-Ti torsion angle (c). The bottom panel (d) shows the number of H_2 molecules that are within 2.2 Å of Ti atoms. It indicates successive desorption of H_2 molecules in the course of the simulation.

both C-C and Ti-C bond distances oscillate around their equilibrium lengths without any indication of instability. Similarly, the Ti-C-C-Ti torsion angle also slowly oscillates around its equilibrium value of 180° and does not show any evidence for Ti-Ti dimer formation for which the torsion angle is supposed to be about 57°. Figure 11(d) shows the number of H_2 molecules that are close to a Ti atom (within a 2.2-Å distance), showing that initially two H_2 molecules are released and then another H_2 molecule is released at around 2.4 ps. Above 6 ps, the number of H_2 fluctuates indicating that the distances are going beyond 2.2 Å more often. Probably if we had run the MD simulation further, we would lose the remaining H_2 molecules that are attached to the Ti atoms.

As a final example, in Fig. 12, we present results from a 10-ps MD run on titanol+$5H_2$ molecules at 500 K. The C-C and Ti-C distances indicate that the bare titanol molecule is stable at this temperature. The C-C-Ti angle shown in Fig. 12(c) indicates that the C-C-Ti bond angle is very soft, exhibiting large amplitude motion. Around 5 ps, Ti actually goes to the middle of two carbon atoms, returning to our original C_2H_4Ti-like configuration. As we discussed in the previous section, these two configurations are almost degenerate. The last panel shows the number of H atoms that are within 2.2 Å of the Ti atom. Three successive constructive desorptions of H_2 molecule are evident.

In summary, our MD results discussed above on different systems indicate that the sandwich configuration of $C_2H_4Ti_2$ is quite stable and can bind H_2 molecules and then release them at elevated temperature. Similarly, $C_2H_4Li_2$ MD results also suggest that Li is another promising option even though the strength of the interactions is at the low side. Finally,

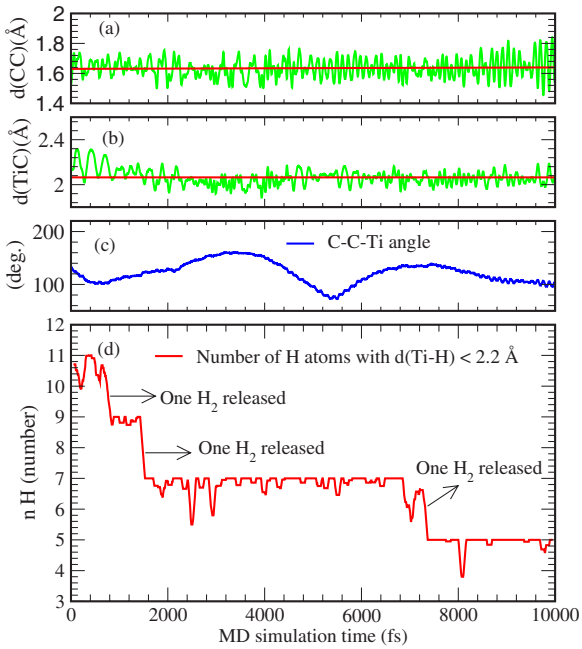

FIG. 12. (Color online) Various quantities (same as in Fig. 11) obtained from MD simulations of the titanol+$5H_2$ system at 500 K.

thanks to MD simulations, we discovered a new configuration, titanol, which is derived from the $C_2H_4Ti+H_2$ system and capable of binding five H_2 molecules and then releasing them at high temperature without breaking down its structure.

VI. CONCLUSIONS

Our conclusions are summarized as follows:

(i) We showed that the C═C bond in ethylene can mimic the double bond in other carbon structures like C_{60}, in terms of binding metal atoms and the hydrogen absorption properties. The small system size of the *M*-ethylene complex allowed us to do very detailed studies such as long MD simulations and reaction path calculations, which were very difficult to perform otherwise. Most of the results that we found, such as H_2 dissociation and titanol formation, should be valid for other Ti-decorated nanostructures.

(ii) For light transition metals, we showed that the initial H_2 absorption could be either molecular with binding energy of ~0.3 eV or it could be chemical by TiH_2 formation with a binding energy of ~1.0–1.5 eV. However, there is a barrier of ~0.25 eV for this process. Since the molecular H_2 has a binding energy of ~0.3 eV, the dissociation could not be observed. Indeed, in our MD simulations, we did not see conversion from $Ti+H_2$ to TiH_2. Instead, we discovered that there is a very-low-energy barrier for the simultaneous dissociation of H_2 and formation of CH bonding (similar to spill-over effect) through the Ti atom. For the case of $C_2H_4Ti+H_2$, this reaction yielded a new molecule which is isostructural to ethanol and can bind five hydrogen molecules with an average binding energy of ~0.4 eV.

(iii) We showed that the sandwich configuration of $C_2H_4M_2$ is quite stable for both transition metals and Li. There are high-energy barriers for the transition to dimer configurations. Our 10-ps MD simulations did not show any evidence for dimerization.

(iv) From our results, it is clear that $C_2H_4M_n$ system could have a very rich phase diagram with different configurations. However, for all the isomer configurations that we have investigated, the complex is always able to bind multiple hydrogen molecules with high absorption capacity. Hence these results suggest that co-deposition of transition/lithium metals with small organic molecules into nanopores of low-density materials could be a very promising direction for discovering new materials with better storage properties.

(v) We note that there are many existing experimental studies of small organic molecules with transition metals in gas phase by mass spectroscopy. In these experiments, the metal atoms are obtained by laser evaporation of bulk metal and then condensed with mixture of Ar and ethylene (or benzene) gas onto a cold substrate. In this way, it was possible to trap $M_x(C_2H_4)_y$ types of complexes in an argon matrix and do spectroscopic experiments on them. We hope that our study will reenergize these studies with the focus on hydrogen absorption properties of these systems. It may be possible to use H_2 rather than Ar to prepare these clusters in a H_2 matrix. Such studies would be very important as a proof of concept and that should be the current emphasis.

ACKNOWLEDGMENTS

We acknowledge partial DOE support from EERE Grant No. DE-FC36-04GO14282 (W.Z., T.Y.) and BES Grant No. DE-FG02-98ER45701 (S.C.). S.C. and E.D. acknowledge partial support from TÜBİTAK under Grant No. TBAG-104T536. We thank J. Curtis and R. Cappelletti for fruitful discussions.

*Electronic address: taner@nist.gov

[1] R. Coontz and B Hanson, in *Towards a Hydrogen Economy*, special issue of Science **305**, 957 (2004).
[2] G. W. Crabtree, M. S. Dresselhaus, and M. V. Buchanan, Phys. Today **57**, 39 (2004).
[3] A. Zuttel, Mater. Today **6**, 24 (2003).
[4] T. Yildirim and S. Ciraci, Phys. Rev. Lett. **94**, 175501 (2005).
[5] T. Yildirim, J. Iniguez, and S. Ciraci, Phys. Rev. B **72**, 153403 (2005).
[6] Y. Zhao, Y.-H. Kim, A. C. Dillon, M. J. Heben, and S. B. Zhang, Phys. Rev. Lett. **94**, 155504 (2005).
[7] S. Dag, Y. Ozturk, S. Ciraci, and T. Yildirim, Phys. Rev. B **72**, 155404 (2005).
[8] B. Kiran, A. K. Kandalam, and P. Jena, J. Chem. Phys. **124**, 224703 (2006).
[9] E. Durgun, S. Ciraci, W. Zhou, and T. Yildirim, Phys. Rev. Lett.

97, 226102 (2006).

[10] *Metal Dihydrogen and Bond Complexes—Structure, Theory and Reactivity*, edited by G. J. Kubas (Kluwer Academic/Plenum, New York, 2001).

[11] L. Manceron and L. Andrews, J. Phys. Chem. **90**, 4514 (1986).

[12] J. Chen, T. H. Wong, Y. C. Cheng, K. Montgomery, and P. D. Kleiber, J. Chem. Phys. **108**, 3909 (1998).

[13] L. Manceron and L. Andrews, J. Phys. Chem. **93**, 2964 (1989).

[14] G. A. Ozin, W. J. Power, T. H. Upton, and W. A. Goddard III, J. Am. Chem. Soc. **100**, 4750 (1978).

[15] M. E. Alikhani and Y. Bouteiller, J. Phys. Chem. **100**, 16092 (1996).

[16] M. Sodupe, C. W. Bauschlicher, S. R. langhoff, and H. Partridge, J. Phys. Chem. **96**, 2118 (1992).

[17] M. R. A. Blomberg, P. E. M. Siegbahn, and M. Svensson, J. Phys. Chem. **96**, 9794 (1992).

[18] I. Papai, J. Mink, R. Fournier, and D. R. Salahub, J. Phys. Chem. **97**, 9986 (1993).

[19] S. Baroni, A. Dal Corso, S. de Gironcoli, and P. Giannozzi, http://www.pwscf.org

[20] G. Mills and H. Jonsson, Phys. Rev. Lett. **72**, 1124 (1994).

[21] G. Henkelman and H. Jansson, J. Chem. Phys. **133**, 9978 (2000).

[22] D. Marx and J. Hutter, in *Modern Methods and Algorithms of Quantum Chemistry*, edited by J. Grotendorst (NIC, FZ Julich, 2000), pp. 301–449.

[23] D. Frenkel and B. Smith, *Understanding Molecular Simulation* (Acaemic Press, New York, 1996).

[24] E. Durgun, S. Dag, V. M. K. Bagci, O. Gülseren, T. Yildirim, and S. Ciraci, Phys. Rev. B **67**, 201401(R) (2003).

[25] E. Durgun, S. Dag, S. Ciraci, and O. Gülseren, J. Phys. Chem. B **108**, 575 (2004).

[26] R. Georges, M. Bach, and M. Herman, Mol. Phys. **97**, 279 (1999).

[27] Y. Zhao, A. C. Dillon, Y.-H. Kim, M. J. Heben, and S. B. Zhang, Chem. Phys. Lett. **425**, 273 (2006).

[28] N. Akman, E. Durgun, T. Yildirim, and S. Ciraci, J. Phys.: Condens. Matter **18**, 9509 (2006).